3 MATHEMATICAL MODELLING

3.1 Preamble

In this chapter, the mathematical modelling of the semi-active hydro-pneumatic spring/damper system is discussed. This includes a description of the different mathematical sub-models, as well as the integration of the sub-models. A complete discussion on the correlation between the measured and simulated results is provided in Chapter 5.

A real gas thermal time constant approach is used to model the hydro-pneumatic springs, while incompressible, inviscid flow is used to model the hydraulic pipe flow. A look-up table, with first order delay, is implemented to approximate the semi-active damper. Two variations of the basic mathematical model were constructed. The first model is used for modelling the characterisation process (Refer to Chapter 4 for characterisation detail). For these simulations the strut is subjected to different displacement inputs and valve switching signals. The damper is not included for these simulations, since no damper was present during the characterisation tests.

The second model simulates a single degree of freedom setup. This model includes the strut, as well as the single degree of freedom mass dynamics. Control signals recorded during the tests are used to switch both the spring and damper valves.

An alternative model to the real gas thermal time constant model (which is quite a sophisticated model) is also briefly discussed in this chapter. This model is based on the anelastic model, discussed in Chapter 2 and is less complicated than the real gas model.

The mathematical sub-models will be discussed separately in the following paragraphs.

3.2 Mathematical sub-models

3.2.1 Hydro-pneumatic spring model

As mentioned previously, a real gas thermal time constant approach is used for modelling the hydro-pneumatic springs. The reason for using a real gas approach is that the pressures and temperatures of the Nitrogen inside the spring are much higher than the critical values (refer to Chapter 2 for a more complete discussion). An ideal gas approach would therefore not be suitable for modelling the spring/damper unit of this study.

The hydro-pneumatic spring model, adapted by Els (1993), from the thermal time constant approach suggested by Pourmovahed and Otis (1990) is applied for the hydro-pneumatic springs. The BWR equation of state (Cooper & Goldfrank 1967) was used to determine the gas pressure.

The way the model approximates the hydro-pneumatic spring characteristics is by solving the gas temperature differential equation, which is a function of gas temperature, ambient temperature, specific volume and time. The model of Els (1993) was re-coded in Matlab/Simulink format and is solved using a fourth order Runge Kutta integration routine (ODE45) in Matlab. Equation 3-1 indicates the temperature differential equation taken from Els (1993).

$$\dot{T}_g = \frac{(T_a - T_g)}{\tau} - \frac{\dot{v}}{C_v}\left[\frac{RT_g}{v}\left(1+\frac{b}{v^2}\right)+\frac{1}{v^2}\left(B_0RT_g+\frac{2C_0}{T_g^2}\right)-\frac{2c}{v^3T_g^2}\left(1+\frac{\gamma}{v^2}\right)e^{-\frac{\gamma}{v^2}}\right] \qquad (3\text{-}1)$$

with

$\dot{T}$ - Change in gas temperature $[K/s]$
T_a - Ambient temperature $[K]$
T_g - Gas temperature $[K]$
τ - Thermal time constant $[s]$
C_v - Specific heat capacity of the gas $[J/kgK]$
$\dot{v}$ - Change in gas specific volume $[m^3s/kg]$
R - Specific gas constant $[J/kgK]$
b, B_0, C_0, c, γ - BWR constants

From the gas temperature the gas pressure is determined, by making use of the Benedict-Webb-Rubin (BWR) equation of state (Cooper & Goldfrank 1967). The BWR equation has previously been shown to give adequate results for hydro-pneumatic spring units of similar volume, pressure and geometry. Equation 3-2 shows the BWR equation of state used to determine the gas pressure.

$$P = \frac{RT_g}{v} + \left(\frac{B_0RT_g - A_0 - C_0/T_g^2}{v^2}\right) + \left(\frac{bRT_g - a}{v^3}\right) + \frac{a\alpha}{v^6} + \left(\frac{c\left(1+\gamma/v^2\right)e^{-\gamma/v^2}}{v^3T_g^2}\right) \qquad (3\text{-}2)$$

with

T_a - Ambient temperature $[K]$
T_g - Gas temperature $[K]$
τ - Thermal time constant $[s]$
C_v - Specific heat capacity of the gas $[J/kgK]$
P - Gas pressure $[Pa]$
R - Universal gas constant $[J/kgK]$
V - Gas volume $[m^3]$
v - Gas specific volume $[m^3/kg]$
$a, A_0, b, B_0, c, C_0, \alpha, \gamma$ - BWR constants for nitrogen gas

Values for the BWR constants of Nitrogen can be found in Cooper and Goldfrank (1967) and are repeated here in metric units: a = 0.15703387, A_0 = 136.0474619, b = 2.96625e-6, B_0 = 0.001454417, c = 7.3806143e-5, C_0 = 1.0405873e-6, α = 5.7863972e-9, γ = 6.7539311e-6

Figure 3-1 displays a schematic representation of the Simulink model of the hydro-pneumatic spring. From this figure it can be seen that the hydro-pneumatic spring model requires one input variable, namely floating piston displacement, while the gas temperature and pressure are the two main outputs of this block.

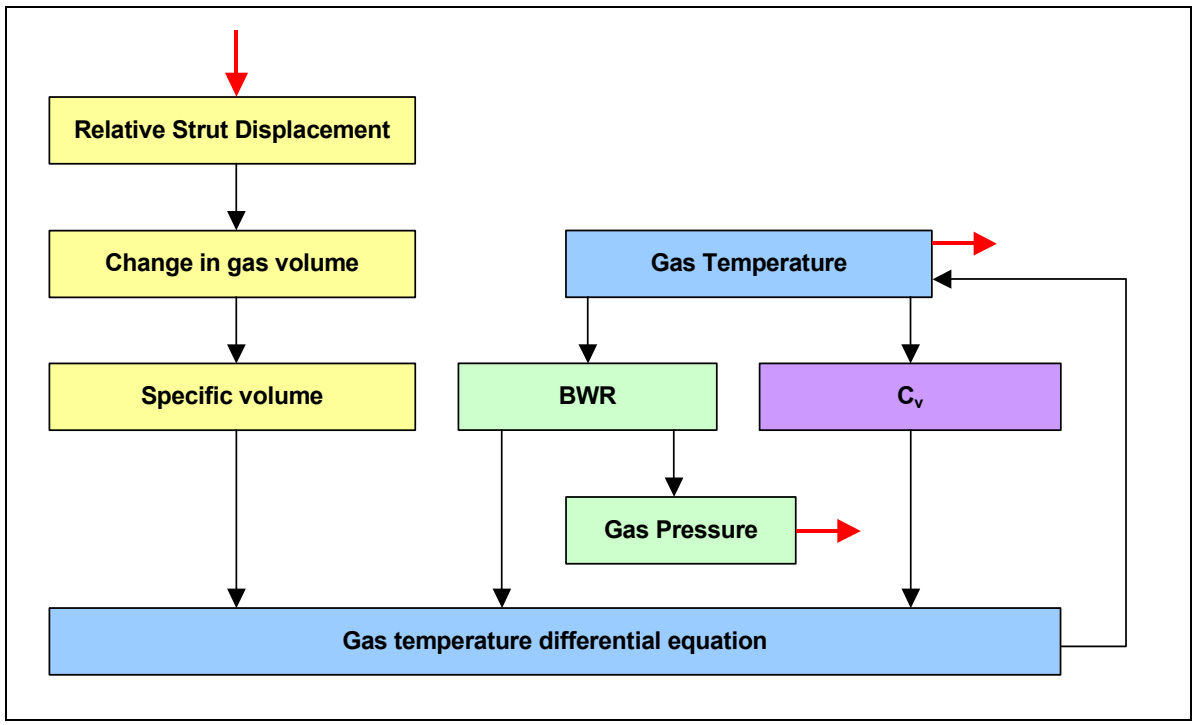

Figure 3-1: Simulink model of the hydro-pneumatic spring

From Figure 3-1, it can be seen that the specific heat capacity is calculated at each time step, as a function of gas temperature. The following equation is used to determine the ideal gas specific heat capacity (Els 1993):

$$C_v^0 = R\left(\frac{N_1}{T_g^3} + \frac{N_2}{T_g^2} + \frac{N_3}{T_g} + (N_4 - 1) + N_5 T_g + N_6 T_g^2 + N_7 T_g^3 + \frac{N_8 y^2 e^y}{(e^y - 1)^2}\right) \quad (3\text{-}3)$$

with

C_v^0 - Ideal gas specific heat capacity $[J/kgK]$
R - Universal gas constant $[J/kgK]$
T_g - Gas temperature $[K]$
$y = \frac{N_9}{T_g}$
$N_1 - N_9$ - Constants (Els 1993)

In the model of Els (1993) the ideal gas specific heat capacity is corrected (for pressure) to obtain the real gas specific heat capacity. It was however found that the ideal gas and real gas specific heat capacities differ by less than 0.0001% for the typical pressures and temperatures encountered in this study. The correction of the ideal gas specific heat capacity was therefore neglected.

A complete breakdown of the hydro-pneumatic spring model is provided in Appendix B.

3.2.2 Hydraulic damper model

The hydraulic damper was only present for the SDOF simulations and not for the characterisation simulations. Since the damper consists of a discrete two-state damper, it was decided to make use of a look-up table, where the damper characteristic can be found by interpolating on one of two graphs. The valve response of the damper valve, as well as the spring valve was modelled as a first order delay, based on measured valve response times. The valve models are discussed in paragraphs 3.2.4 and 3.2.5.

The damper characteristics used for the simulations were determined experimentally, as described in Chapter 4. Figure 3-2 shows the "on" and "off" damper characteristics.

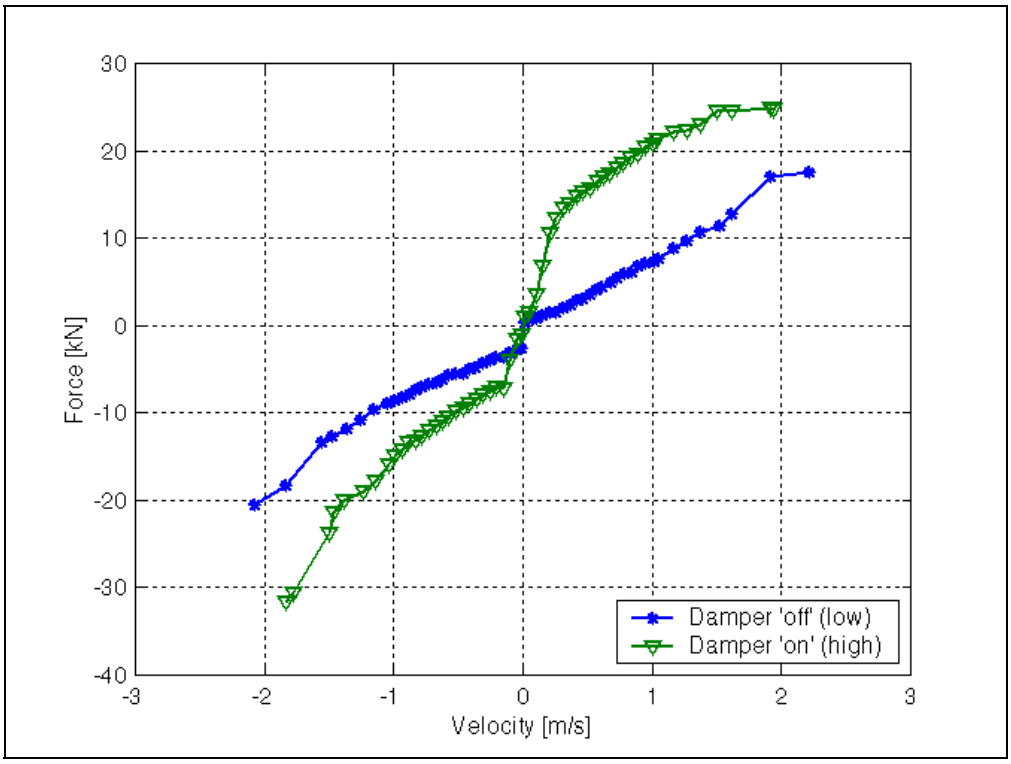

Figure 3-2: Semi-active damper characteristic

A 2D linear interpolation scheme was used to determine the damper force, dependant on the state of the semi-active damper valve, i.e. "on" or "off". Figure 3-3 indicates the Simulink model incorporating the damper look-up for the "on" and "off" states, as well as the damper switching signal input.

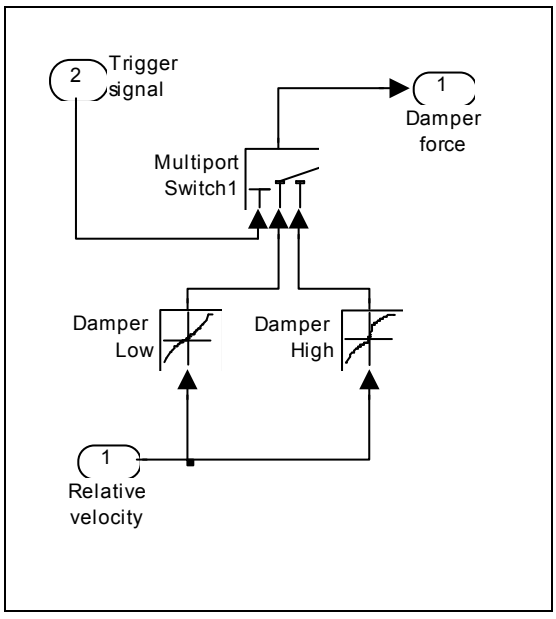

Figure 3-3: Damper model

From this figure it can be seen that both the high and low damper force are calculated continuously, but that only one of these signals are connected to the damper force output signal line at any time. More detail about the damper valve model can be found in paragraph 3.2.4.

3.2.3 Hydraulic flow model

The hydraulic flow was modelled as incompressible, inviscid flow. The elemental equations are derived from first principles and represent the system without the semi-active damper. A complete derivation of the hydraulic flow model is presented in Appendix C. Figure 3-4 shows the Simulink model of the hydraulic flow. The elements of the flow model are shown in blue, while the spring models are orange.

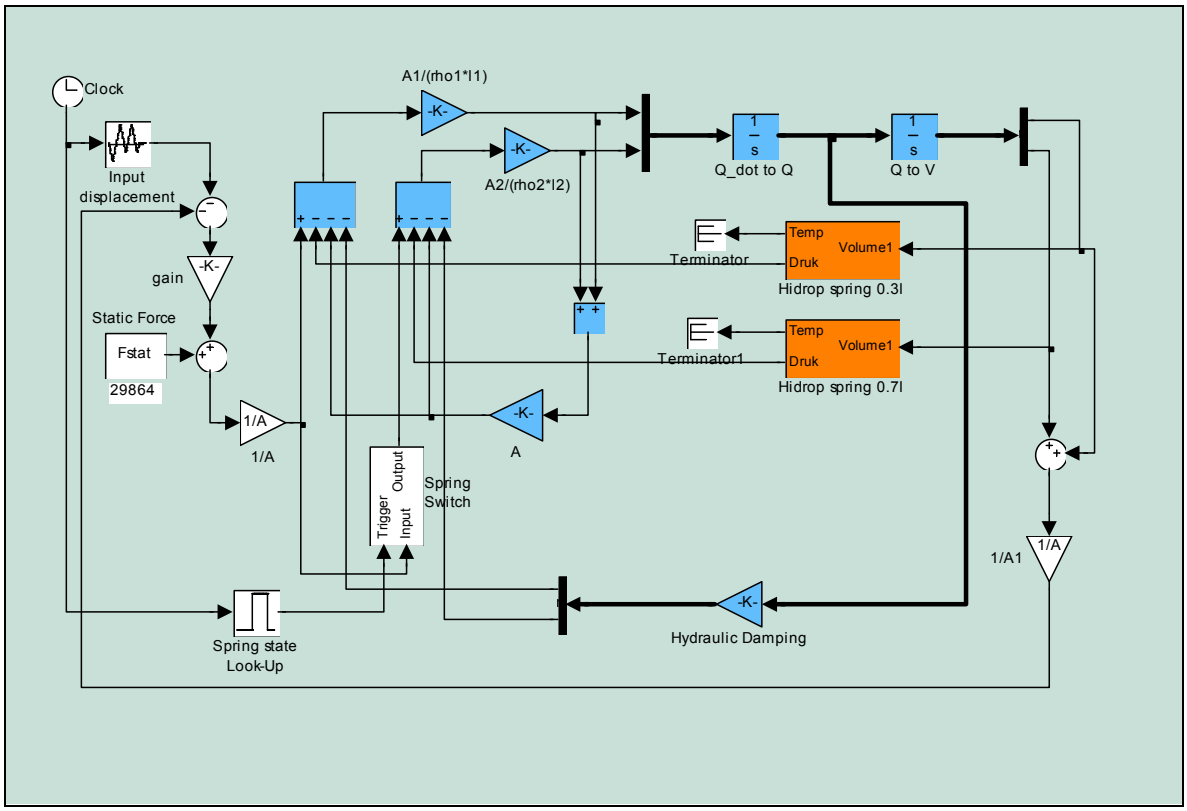

Figure 3-4: Hydraulic flow model in Simulink

From this figure it can be seen that a displacement feedback loop is used to control the input to the parallel hydro-pneumatic springs. This Simulink model determines the change in flow rate to each of the accumulators, which is then integrated twice to obtain the volume. The volumes are fed to the two spring models from which the pressure inside the two accumulators are calculated. Accumulator pressures are then fed back to the summer blocks in order to calculated the new change in flow rate based on the current accumulator pressure and the input signal (pressure).

Also visible in the Simulink model is a gain block called damping. This block was added in order to eliminate resonance between the two accumulators. In practice there are flow losses in the pipes that will damp out the flow exchange between the two accumulators. A constant value was assumed for the damping and was coupled to the flow rate, as is flow losses. The magnitude of the damping constant was determined through trial and error to eliminate high frequency pressure resonance.

3.2.4 Damper valve model

As mentioned previously, the damper valve model is based on a first order delay of the switching signal. The relative strut velocity determines the magnitude of the delay. The delay is calculated by evaluating a polynomial function representing the valve response time as a function of relative velocity. The coefficients of the polynomial function were determined by fitting a parabola to measured damper valve response times. Figure 3-5 shows the measured valve response times and the parabolic fit used in the Simulink model. A definition of valve response time can be found in paragraph 4.5.4 of Chapter 4.

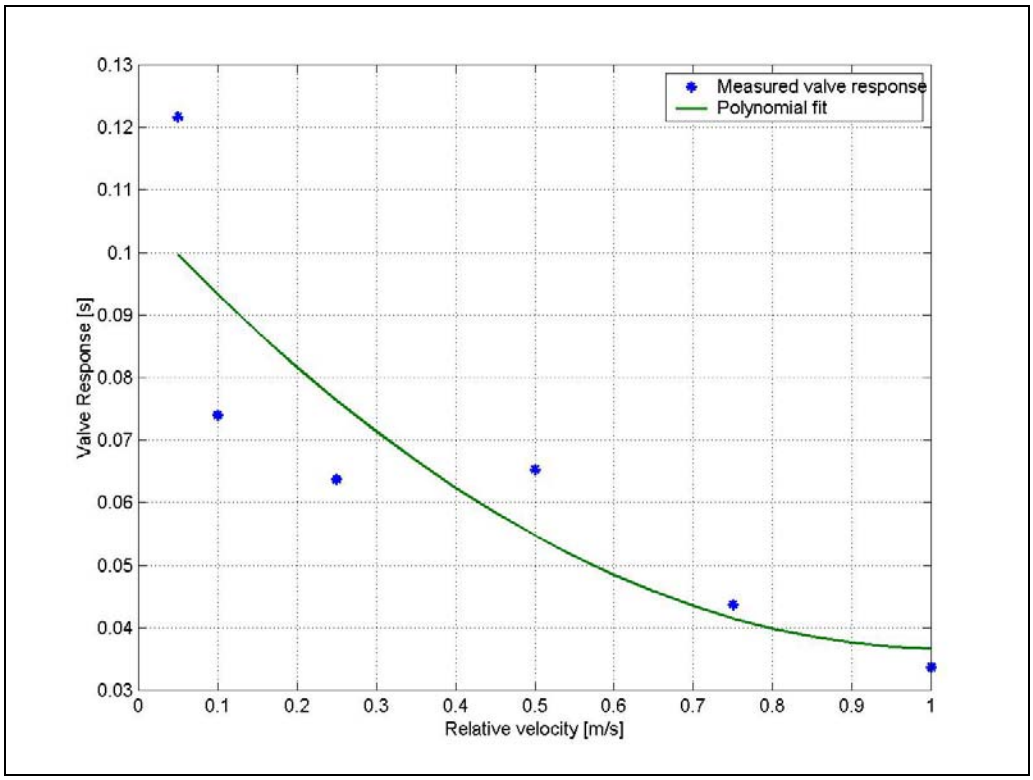

Figure 3-5: Polynomial fit to measured damper valve response data

Figure 3-6 indicates how this model is implemented in Simulink.

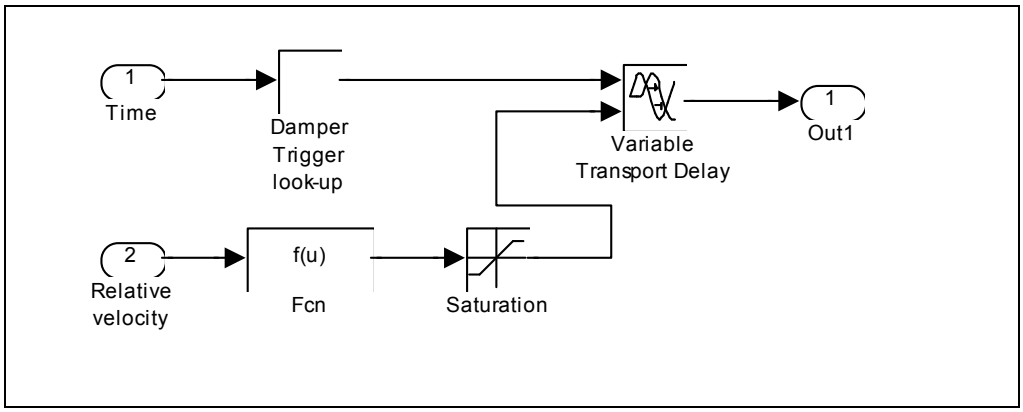

Figure 3-6: Damper valve model

In this figure the look-up table for determining the damper state, the function for calculating the response time, a saturation block and a variable transport delay block can be seen. The purpose of the saturation block is to ensure that only realistic delay values are passed to the variable transport delay block.

3.2.5 Spring valve model

The spring valve model not only incorporates the valve response of the spring valve, but also forms an integral part of the dual spring model. Since the flow rate and volume of each spring is fed back to the model, the flow rate to the isolated accumulator has to be zero. The accumulator volume therefore has to remain constant when the accumulator is disconnected from the hydraulic system. This was achieved by including a spring valve switching module displayed in Figure 3-7. From this figure it can be seen that when the valve is “open” or “off”, the input is directly connected to the output. When the valve is “closed” or “on” the last input value is maintained at the output. The spring valve switch therefore maintains a constant pressure inside the accumulator that is isolated from the rest of the hydraulic circuit.

The spring valve response was incorporated in the same way as the damper valve response. In the case of the spring valve a linear curve is fitted to the measured response data, as can be seen in Figure 3-8. The valve response of the spring valve is supplied as response time versus force difference. The force difference can also be interpreted as a pressure difference in the two accumulators. When the valve is open, the pressure difference is small and the delay is a maximum (approximately 130ms).

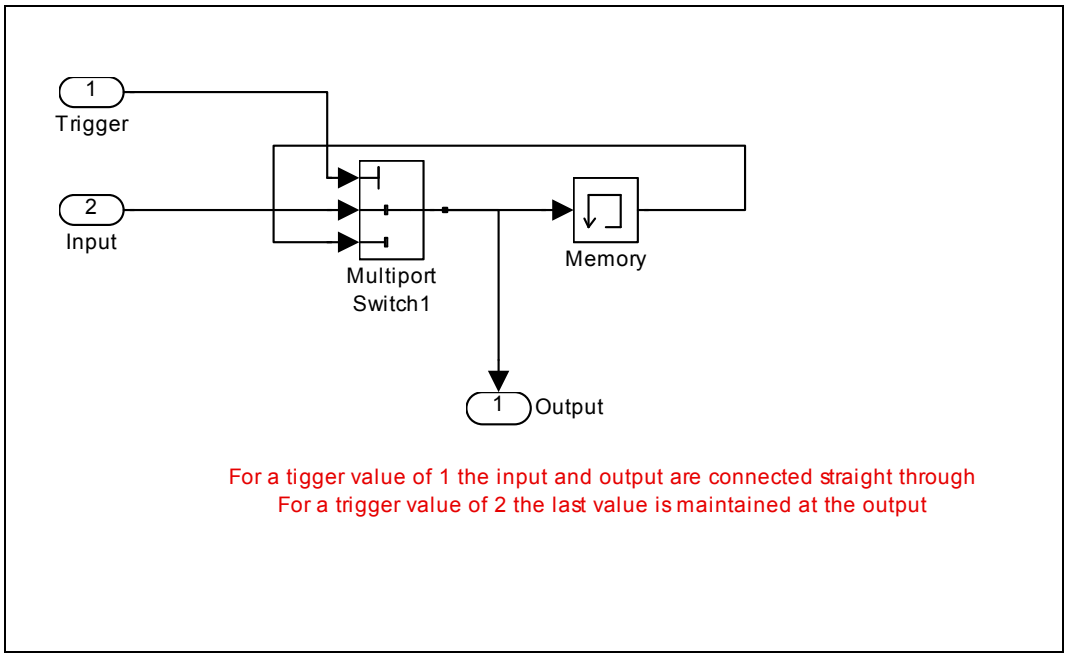

Figure 3-7: Spring valve switching module

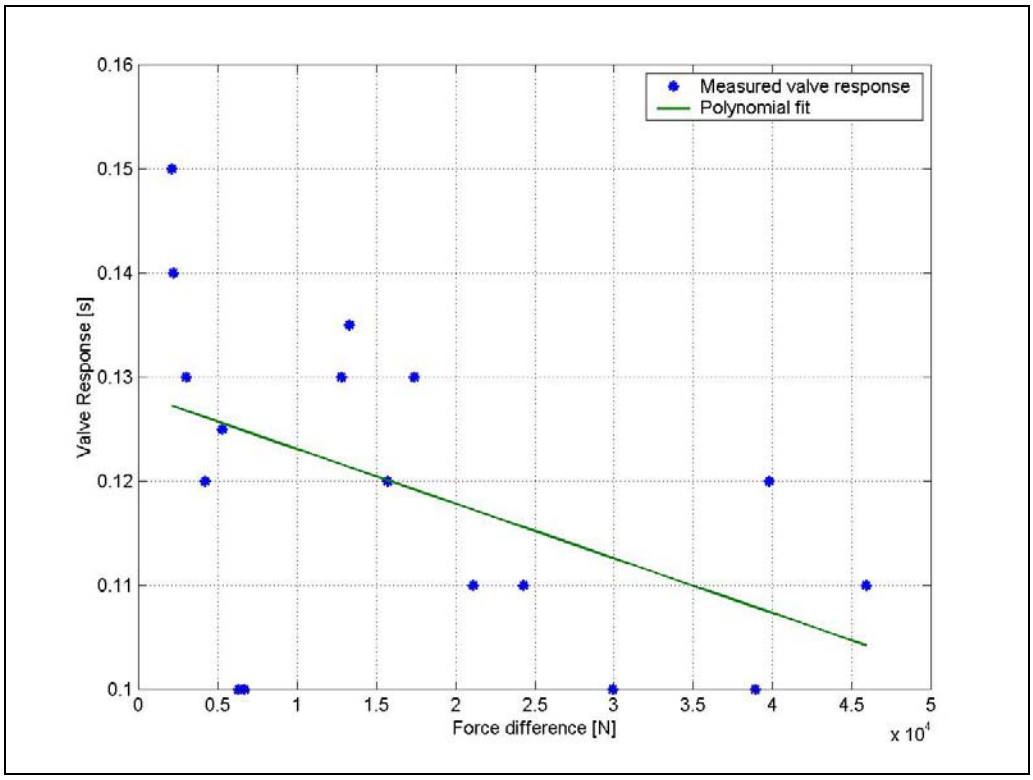

Figure 3-8: Linear fit to measured spring valve response data

Figure 3-9 indicates the spring valve model. From this figure, it can be seen that a look-up table is used to determine the required spring state from the recorded data and that the pressure difference is used to calculate the delay time. The absolute value of the pressure difference is used to eliminate negative response times. The pressure difference is converted to a force

difference. The force difference is then used to determine the valve response time from the linear fit to measured data. A saturation block is included to ensure that realistic valve response times are always fed to the variable transport delay block.

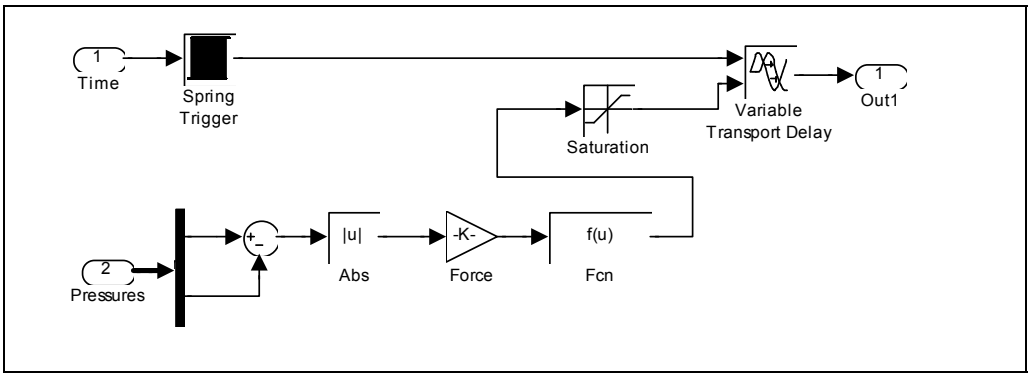

Figure 3-9: Spring valve model

In both the damper and spring valve models, the response delay value is multiplied by 0,5. The reason for this is that the valve response time is defined as the time for the force to rise from 5% to 95% of its final value. The delay therefore has to be only half of this value, since the valve is switched half way between the initial and final time. Figure 3-10 indicates that in practice the valve does not switch immediately, but that the valve was modelled as switching instantaneously, halfway between the start and end time.

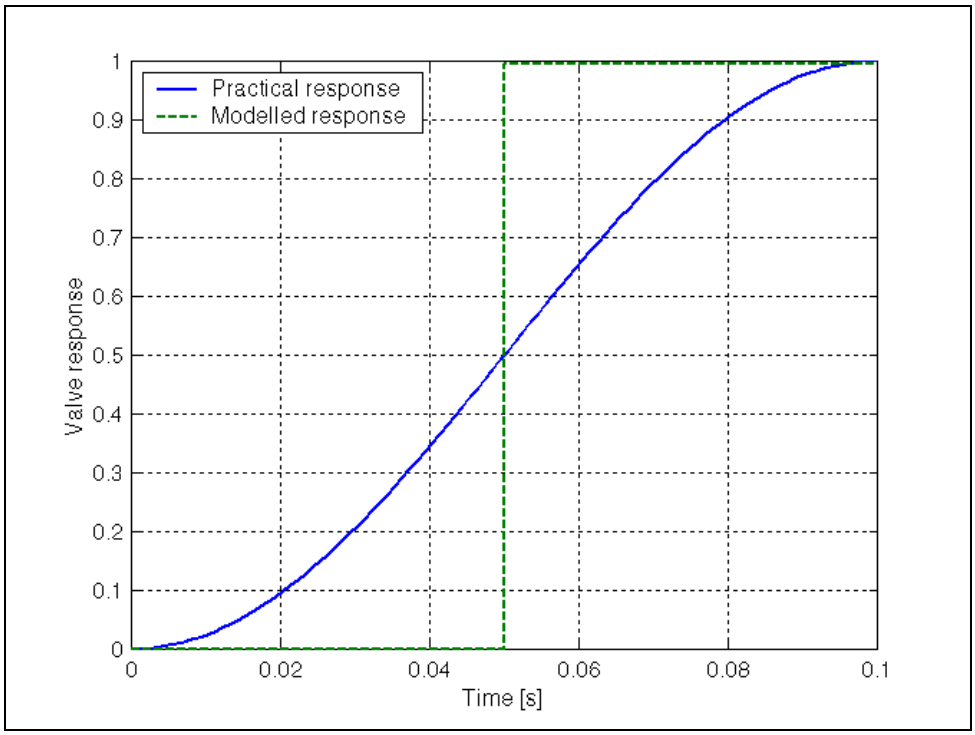

Figure 3-10: Modelling the response delay

3.3 Sub-model integration

The various mathematical sub-models were integrated into a single Matlab/Simulink model. Figure 3-11 shows the complete Simulink model used for the SDOF simulations. From this figure, it can be seen that the mathematical sub-models were included as sub-systems in the Simulink model in order to reduce the complexity of the main model.

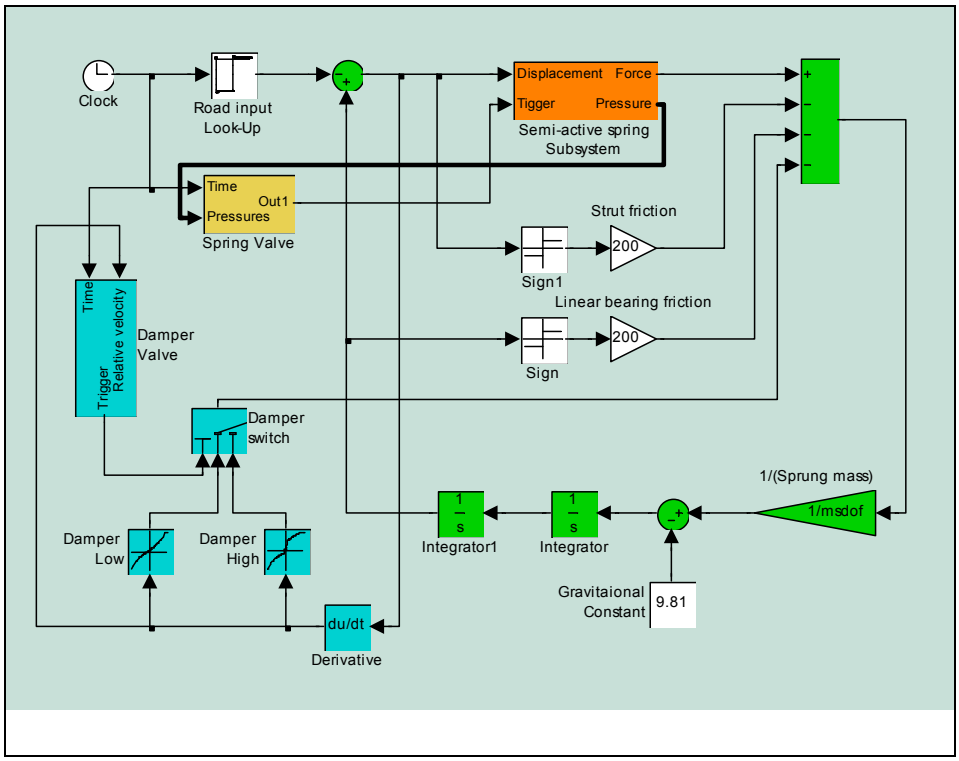

Figure 3-11: SDOF Simulink model

The main SDOF model therefore contains the semi-active damper and valve model (Cyan), the semi-active spring valve model (Yellow), the two spring models contained in the semi-active spring sub-system (Orange), as well as the SDOF sprung mass differential equation (Green). Friction in the linear bearings for the sprung mass, as well as in the strut is also included in the model. The friction was modelled as dry friction with a peak value of 200N. This value was determined through trial and error. The input to this model is the road displacement and the valve switching signals.

3.4 Alternative mathematical model

For basic 2D and 3D vehicle dynamics simulations, a complex mathematical model such as the real gas thermal time constant model discussed in the preceding paragraphs might contain too much detail. A basic anelastic model is therefore included in this chapter as an alternative to the

more complex model. Figure 3-12 shows a schematic representation of the anleastic model. From this figure, it can be seen that the anelastic model consists of a spring in parallel with a spring and damper, which is in series. Through inspection it is possible to see that the basic spring stiffness is supplied by spring k2, while the hysteresis loop will be produced by the series spring and damper combination.

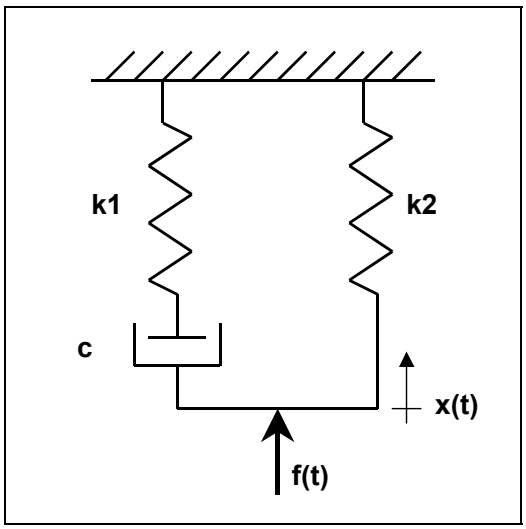

Figure 3-12: Anelastic model for modelling heat transfer in accumulators

Although linear spring and damper characteristics in this model also produce a hysteresis loop, the characteristics are not progressive, as with a hydro-pneumatic spring. It was therefore decided to use a polytropic process to model the main spring. Since the volume and pressure of the accumulators are known, the one unknown parameter (for the main spring) is the polytropic constant. In order not to over complicate the model, linear characteristics were assumed for the series elements. Equation 3-4 shows the formula used to calculate the spring force (F) as a function of displacement (x).

$$F = \frac{kA}{(xA)^n} \tag{3-4}$$

with

F - Spring force [N]

k - Constant (function of static volume and pressure)

A - Accumulator floating piston area [m^2]

x - Floating piston displacement [m]

n - Polytropic exponent

During the process of determining the values of k1 and c, it was found that for the accumulators used in this study, with a thermal time constant of approximately 6*s*, the thermal damping is negligible for frequencies of interest in vehicle dynamics studies. The polytropic constant is however a function of excitation frequency and amplitude, therefore the characterisation real gas model discussed in paragraph 3.2.1 was used to determine the polytropic exponents. Figure 3-13 shows a graph in linear and log scale of the polytropic exponent determined in this way. For this "characterisation", the values for k1 and c were kept constant at 3e3*N/m* and 2.5e3*Ns/m*, however it should be possible to neglect the series spring and damper altogether, since there is very little thermal damping present at the frequencies indicated in Figure 3-13.

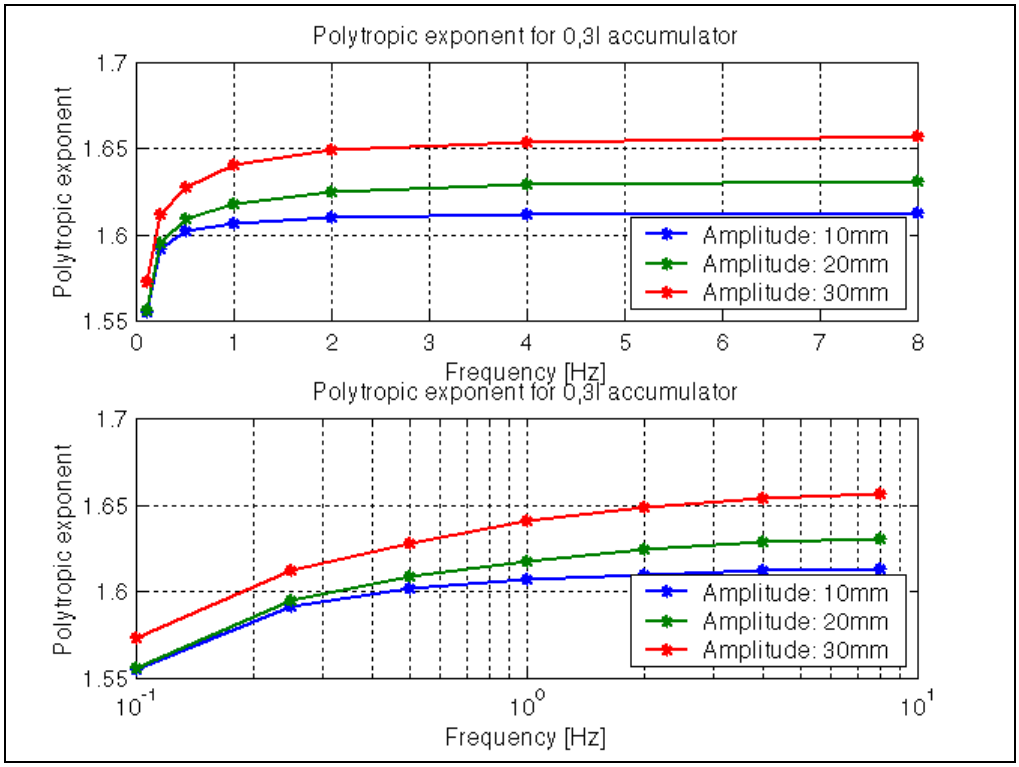

Figure 3-13: Polytropic exponent as a function of excitation frequency and amplitude

Table 3-1 contains several figures, which compares the force vs. displacement characteristic of the real gas thermal time constant and anelastic model. Three excitation frequencies, namely 0.25Hz, 1.0Hz and 4.0Hz are shown for excitation amplitudes of 10mm, 20mm and 30mm. From this table, it can be seen that the hysteresis loop is only really visible for an excitation frequency of 0.25Hz, which is below any rigid body or wheel hop natural frequencies found on wheeled vehicles. It is therefore valid to disregard thermal damping when modelling the hydro-pneumatic spring.

Table 3-1: Comparison between Real gas and Anelastic model

	10mm	20mm	30mm
0.25*Hz*	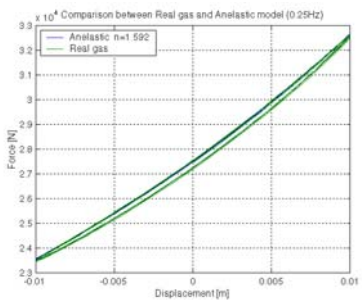	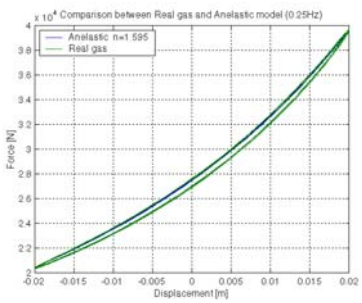	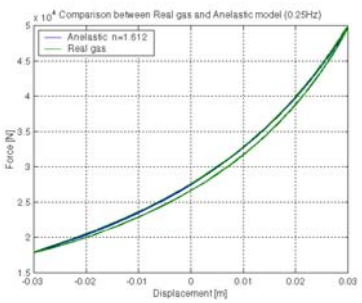
1.0*Hz*	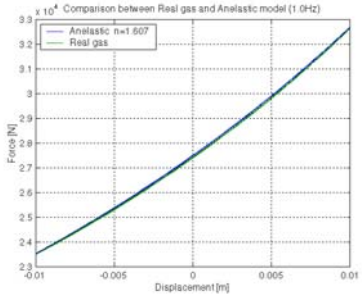	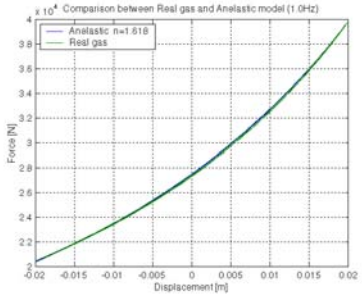	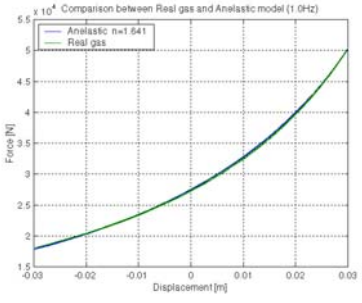
4.0*Hz*	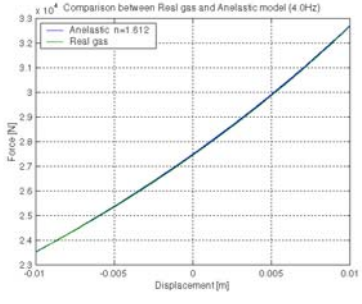	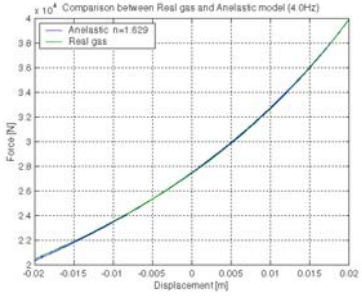	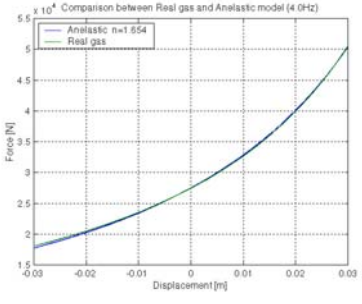

Although the Anelastic model was not evaluated in the semi-active spring, it should be quite easy to generate a semi-active spring model based on a mechanical model using force balance. Figure 3-14 shows a schematic layout of such a configuration. The displacement of spring k1 can be selectively held fixed, making it the accumulator that is being closed of by the valve, while the beam ensures that equal force (pressure) is exerted by both springs. It is recommended that the semi-active anelastic model be further investigated and thoroughly correlated with measured data.

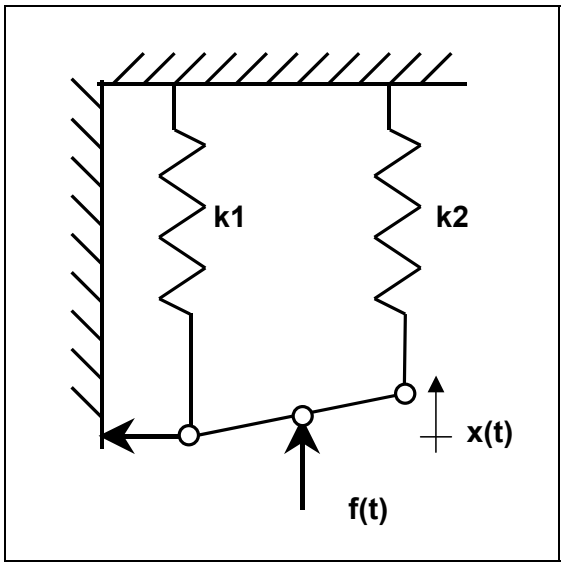

Figure 3-14: Semi-active anelastic spring model

3.5 Simulations

As mentioned previously, all the simulations were performed using Matlab/Simulink. The ODE45 (Fourth order Runge-Kutta) numerical integration algorithm was used for all simulations and an error tolerance of $1e^{-6}$ was prescribed. A 333*MHz* Pentium II computer with 64*Mb* RAM was used to solve the mathematical models. The CPU times for the full SDOF model were between 5 and 10 minutes for approximately 10s of real time input. The anelastic model runs in a matter of seconds for a simulation time of 100*s*.

3.6 Closing

Sub-systems such as the damper, spring, valve etc. are modelled as separate sub-systems and then combined to form the main model. This approach reduces the main model complexity and simplifies the debugging process. The models consist of previously developed models (hydro-

pneumatic spring), look-up tables (damper), empirical models (valve models) and models derived from first principles (hydraulic flow models).

****